Available online at www.sciencedirect.com
ScienceDirect
Journal of the European Ceramic Society 31 (2011) 2551–2558
www.elsevier.com/locate/jeurceramsoc

Influence of powder morphology on properties of ceramic injection moulding feedstocks

Anne Mannschatz*, Axel Müller, Tassilo Moritz

Fraunhofer Institute for Ceramic Technologies and Systems, Winterbergstrasse 28, 01277 Dresden, Germany

Available online 21 February 2011

Abstract

The powder–binder-mixture is the most critical aspect in the injection moulding processing chain, because the feedstock properties determine the success of the following steps, i.e. excellent flowability in the injecting phase and high green strength during debinding. Therefore, nearly spherical particles which pass each other easily in the feedstock stream are advantageous. The applicable particle size is limited in order to reach high solids loadings which are connected with the specific powder surface. According to this, in this study a very unfavourable powder was introduced into a feedstock. The investigated β-alumina powder consists of plate-like primary particles and has a specific surface of 25 m^2/g. During mould filling the particles orient in the feedstock stream which affects the debinding and sintering behaviour and is the source of defects. The influence of the plate-like shape on defect formation is demonstrated in comparison to spherical-shaped particles having the same specific surfaces.

Keywords: A. Injection moulding; B. Platelets; Defects; Beta-alumina

1. Introduction

Producing advanced ceramic components by powder injection moulding makes complex shaped parts available for novel applications in large quantities since finishing expenses of sintered parts are minimized. In order to ensure defect-free parts the whole process has to be controlled precisely because in each step sources of defects can be implemented which possibly remain undiscovered until the end of the processing chain. Therefore the composition of the powder–binder-mixture, the feedstock, is the most critical factor since it defines the processing conditions, i.e. mixing, flow and debinding behaviour.

The aim of developing a feedstock is to reach high solids loadings in order to provide high green densities for sintering. But this is constrained by the increasing feedstock viscosity.[1] The flow behaviour is defined by the interactions of particles and polymer matrix. During injection the particles have to pass each other by translation and rotation which is enabled by a thin polymer film on the solids surface. Easy gliding is supported by low binder viscosity, good wetting behaviour and complete coating of the powder surface. Agglomerates shall be destroyed during compounding to eliminate enclosed pores and avoid large irregular shaped compacts that act as obstacles and increase flow resistance.[2,3] In terms of flow behaviour the ideal powder should consist of separated spherical particles which exhibit the highest degree of freedom for motion in a stream. At the same time the surface to volume ratio is minimized allowing the reduction of the binder fraction. With respect to debinding some irregular particle shape is favourable because it offers a better shape stability of the particle packing when the binder softens during heat treatment.[4]

Unfortunately, real powders seldom match the ideal and deviate from spherical shape or have large specific surfaces. As known from polymer injection moulding anisometric particles will orient in a shear field.[5,6] In fibre,[7] talc[8] or clay[9] reinforced plastics this causes anisotropic mechanical and thermal properties which have to be taken into consideration during the design phase of a new component. In ceramic processing this affects the quality of the components in particular because the green parts have to undergo thermal treatment. Already in green state internal stresses are caused by stretched polymer chains which have to arrange between the particles and are hindered to gain their natural confirmation if the particles force a certain direction.[10,11] At elevated temperatures the molecules will relax and drag the particles along. Since the particle packing defines the densification behaviour during, sintering inhomogeneities generate

* Corresponding author.
E-mail address: Anne.Mannschatz@ikts.fraunhofer.de (A. Mannschatz).

0955-2219/$ – see front matter © 2011 Elsevier Ltd. All rights reserved.
doi:10.1016/j.jeurceramsoc.2011.01.013

differential shrinkage and thereby defects or distortion. In injection moulding, as in other ceramic shaping technologies,[12] it was observed that the particle orientation depends on the flow direction.[13,14] Due to the dependence of the particle packing from the flow profile the shrinkage can differ in flow direction from 20% in the middle of the cross-section to only 15% near the surface.[15] Clearly, this effect is pronounced by particles with high aspect ratios as they are present in the investigated powder.

2. Experimental

2.1. Materials

Two alumina powders were used in this study. The β-alumina (Calsitherm, Germany) has a specific surface of 25 m^2/g. Its primary particles are platelets which are agglomerated in structures having a mean diameter of 5.5 μm. The platelets are about 20 nm thick, their lateral dimension is in the range of 0.5–4 μm (Fig. 1a). In order to evaluate the influence of particle shape on the flow behaviour, as second powder an α-alumina (Baikowski, France) was chosen. The particles are round shaped with diameters below 100 nm and the powder has a specific surface of 20 m^2/g. Taking the densities of both powders into account the specific surfaces can be related to the volume and show very similar values (Table 1). Both powders are still under development and are not commercially available, yet.

Due to the large surface and small particle size low viscosity polymers had to be employed in the binder system. As major components low density polyethylene and paraffin wax were applied. Additionally micronized amide wax was added whose small particle size (d_{50} = 6.5 μm) is beneficial in mixing with fine powders. Stearic acid was used as surfactant. Characteristical data of the organic components are summarized in Table 2.

2.2. Sample preparation

After heating the powder at 120 °C for removing moisture a portion was mixed with the binder in a double Z-blade kneader (LKII, Linden, Germany) at 160 °C. The premix was then compounded and granulated on a shear roll compactor (BSW 135-1000, Bellaform, Germany). Final solids loading were achieved by stepwise addition of the residual powder.

The feedstock compositions are described in Table 3. At a solid content of 47 vol.% two binder formulations were tested

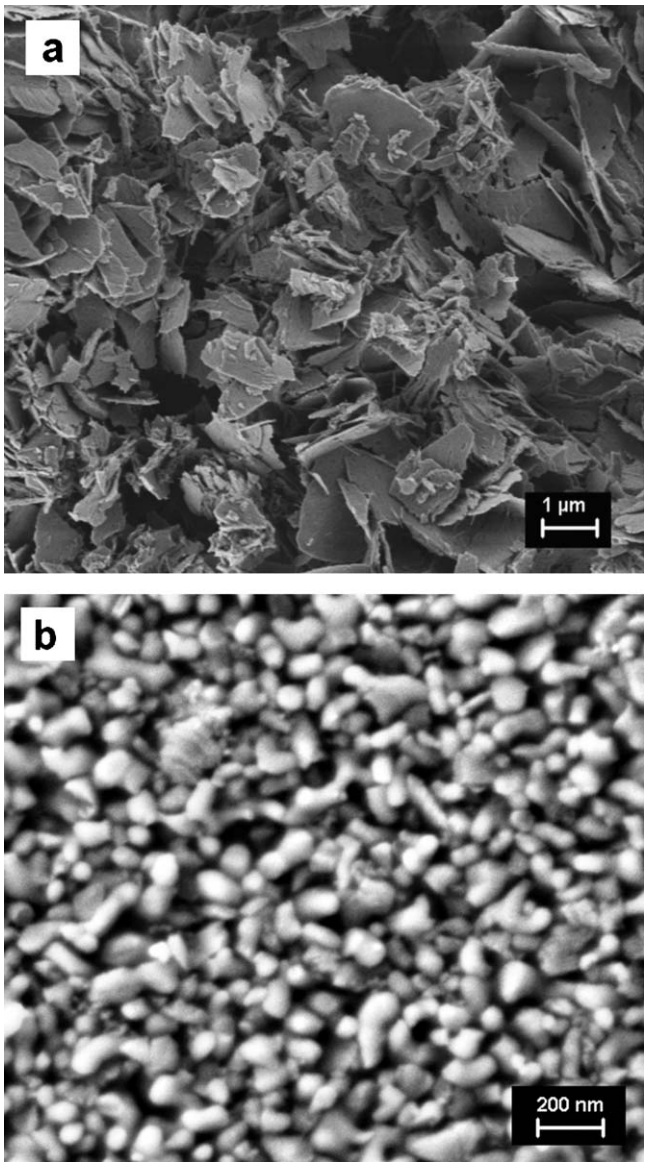

Fig. 1. SEM-images of (a) β-alumina powder and (b) α-alumina powder.

Table 1
Powder properties.

Powder	β-Alumina	α-Alumina
Morphology	Platelets	Round shaped
Spec. surface (m^2/g)	25	20
Spec. surface (m^2/cm^3)	80	79
Density (g/cm^3)	3.19	3.98

Table 2
Properties of binder components.

Binder component	Melting temperature (°C)	Density (g/cm^3)
Low density polyethylene	81	0.91
Paraffine wax	51	0.77
Micronized amide wax	130	1.00
Stearic acid	69	0.94

Table 3
Feedstock composition.

Feedstock	Powder	Solids loading (vol.%)	Ratio of major binder components LDPE:PW[a]
Beta-1–47	β-Alumina	47	9:5
Beta-2–47	β-Alumina	47	1:1
Beta-2–48	β-Alumina	48	1:1
Beta-2–50	β-Alumina	50	1:1
Alpha-2–55	α-Alumina	55	1:1

[a] LDPE: low density polyethylene, PW: paraffine wax.

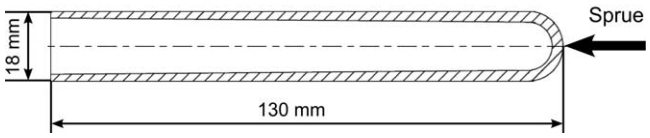

Fig. 2. Green dimensions of sample geometry: tube with closed cap, the position of the sprue is denoted by an arrow.

for the β-alumina which differed in polyethylene to paraffin wax ratio. Within the chosen binder system the powder fraction was increased to 48 vol.% and 50 vol.%, respectively. For the α-alumina a solids loading of 55 vol.% could be achieved with binder composition 2.

Injection moulding was carried out on an Arburg 370C injection moulding machine (Arburg, Germany) at a feedstock temperature of 160 °C and a mould temperature of 60 °C. The formed part was a tube which was closed on one side by a cap (Fig. 2). The sprue was located at the center of the cap. The heating channel was surrounding the tube in helical loops. The core forming the inner tube hole was not heated. Due to the rather long flow length the design was highly demanding for the feedstock because very good flowability is required for complete filling.

For thermal debinding the samples were embedded in a coarse grained alumina powder and carefully heated to 600 °C within 56 h. Afterwards the parts were sintered at 1600 °C for 2 h.

2.3. Characterization methods

The rheological behaviour of the prepared feedstocks was characterized by high pressure capillary rheometry (RH10, Malvern Instruments, Germany) at 160 °C. The capillary diameter was 1 mm with a length of 16 mm. The apparent shear rate was increased stepwise from 50 to 5000 s^{-1}. End effects were accounted for applying the Bagley correction by simultaneous measuring a die with the same diameter and 0.25 mm length. Non-Newtonian flow characteristics of the feedstocks were considered by applying the Rabinowitsch–Weissenberg approach.

During feedstock preparation strong shear forces act on the feedstock which may affect particle shape and dimensions. SEM images of the debinded feedstock granules were used to study the particles after feedstock processing.

In order to analyse the defect development in the injection moulded parts samples were observed after each process step; in green, debinded and sintered state by X-ray computed tomography (CT Compact, Procon X-Ray, Germany). This non-destructive testing method allows scanning a quite large volume to localize internal defects. A tube segment with a length of approximately 20 mm was investigated with a spatial resolution of 27 μm voxel size. During the measurement the sample was rotated in 0.9°-wide steps for 400 projections. The X-ray source was operated at 120 kV and 100 μA and the detector was a 16 bit flat panel detector with 1024 × 1024 pixel. The 3-dimensional images were evaluated according to defect size and orientation.

The microstructure of the sintered parts was investigated on polished surfaces. The cut was carried out perpendicular to the flow direction to study particle orientation.

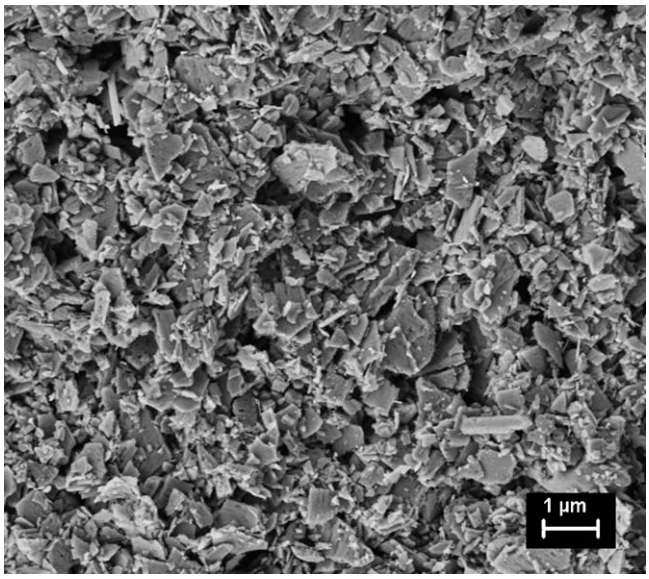

Fig. 3. Surface of a debinded feedstock granule showing β-alumina particles in the feedstock after the compounding process.

3. Results

3.1. Feedstock preparation

The challenge of every feedstock production is accomplishing a homogeneous distribution of powder in the binder matrix. This includes the destruction of agglomerates to gain individualized particles in order to improve their mobility under flow. The shear roll compactor is a suited machine to fulfill this task, because it generates strong shear forces. It consists of two counter-rotating rolls with a distance of 0.5 mm. In the gap the feedstock piles up and internal streams develop. The particle agglomerates get in contact and the relative movement causes friction. The intense shearing overcomes the attractive interparticular forces so that the solid surface can be coated.

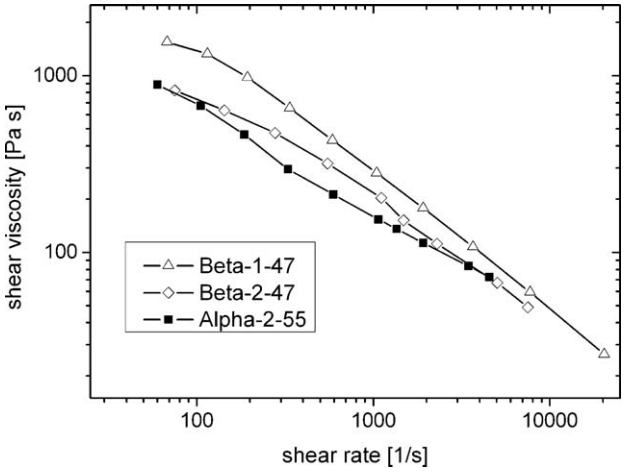

Fig. 4. Viscosity of the feedstocks containing 47 vol.% β-alumina using binder formulations 1 and 2, respectively, compared with a feedstock containing 55 vol.% α-alumina.

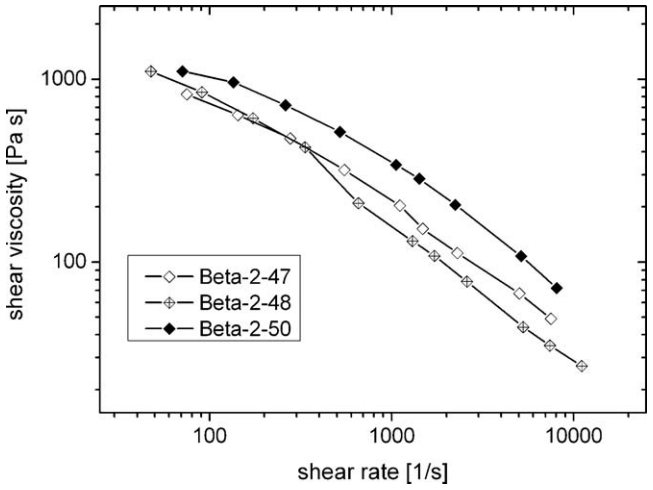

Fig. 5. Viscosity of feedstocks containing β-alumina and binder formulation 2 at different solids loadings.

By precise adjustment of rotational speed, temperature and amount of added powder all feedstock formulations could be prepared successfully and shaped into granulates suited to feed the injection moulding machine. SEM images showed that agglomerates were destroyed and primary particles were separated. While the particle size of the spherical α-alumina kept unaltered the particle size of the β-alumina decreased to typically 0.25–0.5 μm (Fig. 3). This milling effect was caused by the interactions of the platelets in the flowing stream within the shear roll gap. Because the particles orient along the flow lines the platelets are forced to change direction sharply in the pile-up stream. They collide frequently and due to their thin thickness they break. Thus, the specific powder surface which was measured on debinded granules grew to 26.5 m^2/g.

3.2. Flow behaviour of injection moulding feedstocks

As an important parameter the viscosity helps to evaluate the flow performance and to select promising feedstocks for further experiments. In Fig. 4 the shear rate dependent viscosities of the two tested binder formulations for β-alumina at 47 vol.% are shown. Although the feedstocks Beta-1–47 and Beta-2–47 contain both the same binder components and powder content the viscosity of the feedstock with binder formulation 1 is nearly twice as high as for binder composition 2 especially at low shear rates. The higher paraffin content is responsible for the good flowability of Beta-2–47. Since paraffin has an extremely low viscosity it reduces the mixing viscosity of the binder matrix. With this binder system it was possible to increase the solids loading. As a result the viscosity increases as displayed in Fig. 5 which is caused by the intensified particle interactions. Injection moulding experiments showed that the mould could be filled completely at powder contents of 47 and 48 vol.%. At 50 vol.% the feedstock froze before reaching the full cavity length.

The investigated α-alumina which has the same specific surface could be loaded up to 55 vol.% with binder formulation 2. In this case the viscosity (Fig. 4) was similar and at intermediate shear rates even lower than for the β-alumina with only 47 vol.%. Consequently, flawless α-alumina samples could be shaped.

The reason for this observation is the particle shape. The plate-like structure of the β-alumina raises the feedstocks resis-

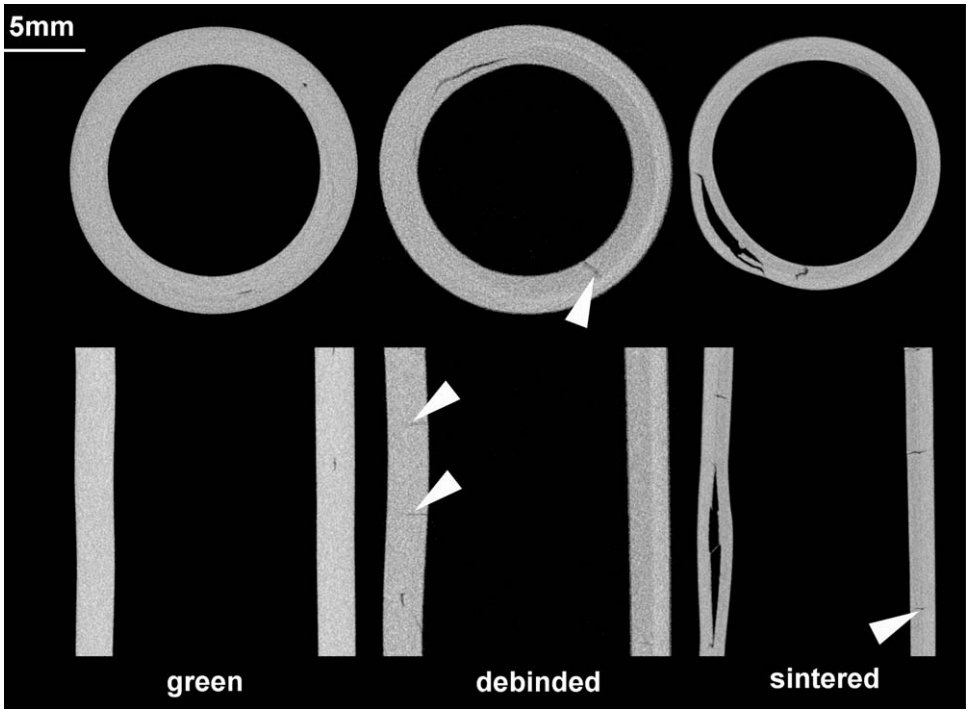

Fig. 6. CT-images of samples in green, debinded and sintered state; planes in cross-sectional (upper row) and longitudinal direction (lower row), radial cracks which grow from the inner wall and end at an internal boundary are marked.

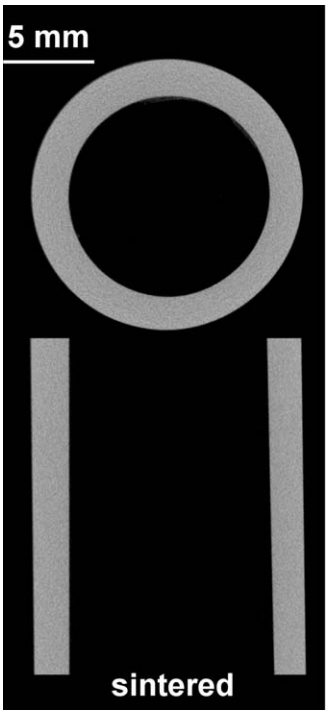

Fig. 7. CT-images of sintered α-alumina sample; planes in cross-sectional and longitudinal direction.

tance against deformation since the particles hinder each others motions in the crowded stream of particles. Especially rotation is restricted because the particles block each other. Powders with spherical shape not only are limited to translateral movement, but can also rotate easily. This enhances the achievable solids content. On the other hand, the relatively low solids loading of the β-alumina will evoke problems in subsequent process steps, i.e. lacking form stability during debinding, potential anisotropic shrinkage.

3.3. Defect formation

The injection moulded β-alumina samples at 47 and 48 vol.% solids loading had no obvious external flaws. However, examination by computed tomography revealed some internal defects. In Fig. 6 planes of CT measurements are presented in cross-sectional (upper row) and longitudinal (lower row) direction. The defect formation can be followed over the three process stages. In the green sample, some elongated voids are located in the middle of the tube wall. During debinding cracks grew circumferentially from these initial defect sites. Additionally, radial cracks formed at the inner wall side and propagated until the middle of the wall. The cracks, all having the same length, seem to end at a defined boundary. In the sintered part the defects expanded, but the radial cracks still stopped inside the wall. At some sites blisters occurred which were also visible from outside. There, inner and outer layer delaminated along the circumference. In contrast, the samples made with the α-alumina powder were defect-free even after sintering (Fig. 7).

SEM investigations of the microstructure (Figs. 8 and 9) explain the appearance of defects. While the α-alumina has a homogeneous microstructure over the complete cross-section (Fig. 9) the tube wall of the β-alumina in Fig. 8a shows a porosity gradient. Large voids have been formed at the inner side near to the core of the tool. Smaller, fine distributed pores are located at the outer side. Elongated grains are visible which still reflect the original particle shape (Fig. 8b). Since they brace each other in a house-of-card-like structure, direct contact to form close packed stacks is inhibited and between the grains likewise elongated voids remain. This shows that the platelets have been aligned in the mould filling phase along the flow direction. The situation at the inner wall is different. In Fig. 8c the grains as well as the pores are larger which points out that the particles were not cut perpendicularly, i.e. they lie in another direction than at the outer side. The boundary between both regions is approximately in the middle of the tube wall.

4. Discussion

The comparison of the samples of both powder types points to the huge influence the particle shape has on the moulding process. The defect-free α-alumina parts confirm that the developed binder system is suited for powders with high surface. That means that the defect formation is strongly related to the particle morphology and the observed defects have their origin in the particle orientation which develops during the mould filling phase.

In contrast to the spherical particles of α-alumina, the β-alumina platelets have a preferential direction when they move in a flowing stream. To reduce flow resistance they orient parallel to the shear layers. During the filling phase the heat is conducted from the feedstock into the mould walls. Therefore frozen layers form in direct contact with the wall. Hence, the channel width for the molten feedstock narrows. In extreme cases, as observed for Beta-2–50, the remaining channel closes and the feedstock front stops before the cavity is completely filled. In a homogeneously heated tool the frozen layers would be equally thick at all sides. In the applied tool, however, the core forming the hole of the tube is not heated. This implicates a deviating temperature gradient for the inner and outer wall which involves asymmetric thicknesses of the solidified layers.

In order to understand the failure behaviour the mould filling for this specific geometry needs to be analysed. Below a possible scenario is introduced which illustrates and explains the filling process. In Fig. 10 the propagating flow front and the current particle orientation is sketched near the gate and in a longitudinal cut through the tube wall. At the moment when the feedstock enters the cavity through the gate (Fig. 10a) it can potentially expand into the whole cavity. But since ceramic feedstocks tend to jetting it impinges onto the cold core as a stream. Because of the sharp flow direction change the particles do not have time to reorientate. Due to rapid cooling the feedstock solidifies almost immediately and preserves the orientation of particles as they have been in the sprue. The progressing feedstock which is shown in Fig. 10b then glides onto the deposited material and creates an internal interface. Due to the differing frozen layers an asymmetrical fountain flow develops in which the particles are oriented in flow direction. When the molten feedstock reaches

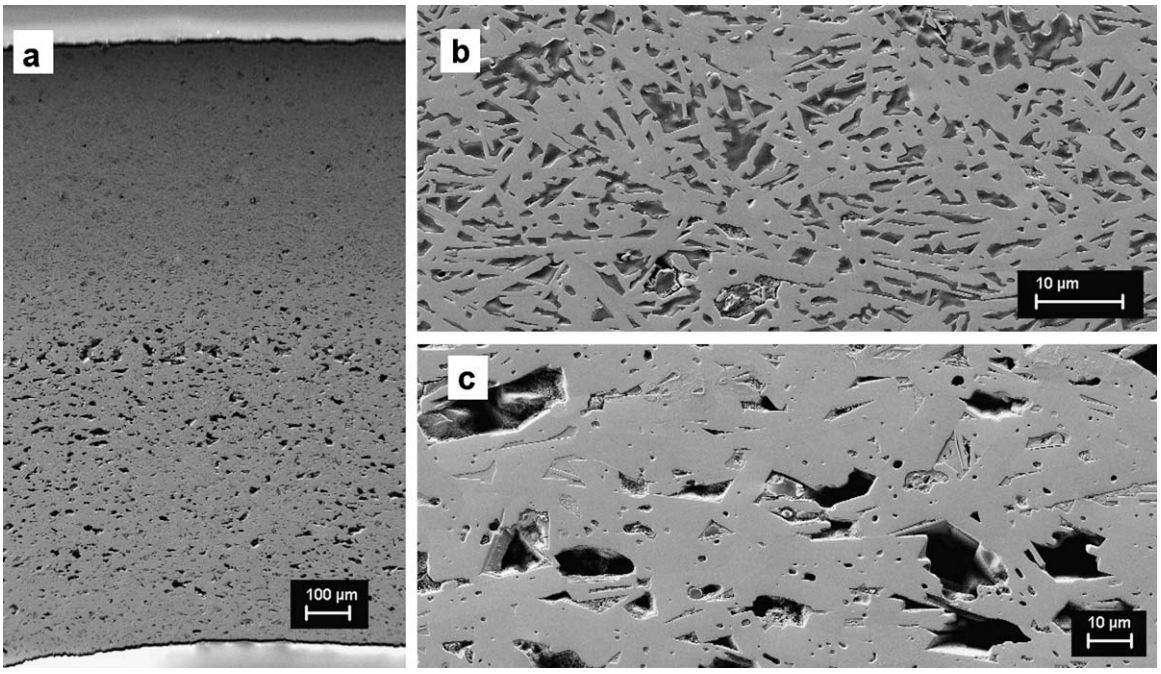

Fig. 8. Microstructure of a sintered β-alumina sample: (a) cross-section through the tube wall, (b) detail at outer side of the wall, and (c) detail at inner side of the wall.

the end of the frozen region the melt expands and the particles tilt into the new direction. Then, the feedstock cools rapidly and the particle orientation is retained. At the end of filling the present particle orientation pattern becomes fixed as two regions orientated parallel and almost perpendicular to flow direction.

This green microstructure influences the following processing steps, because the sample behaves anisotropically. During debinding the binder softens and internal stresses in the polymer matrix are released. Usually, the particles can respond by migration or rotation. Thereby they reduce the particle interspace and get in contact with their neighbours.[16,17] In the plate-like powder this movement is limited since the particles are hindered to rotate and can only move laterally. Moreover, the extent of dislocation depends on the amount of interspace. Thus, the linear shrinkage

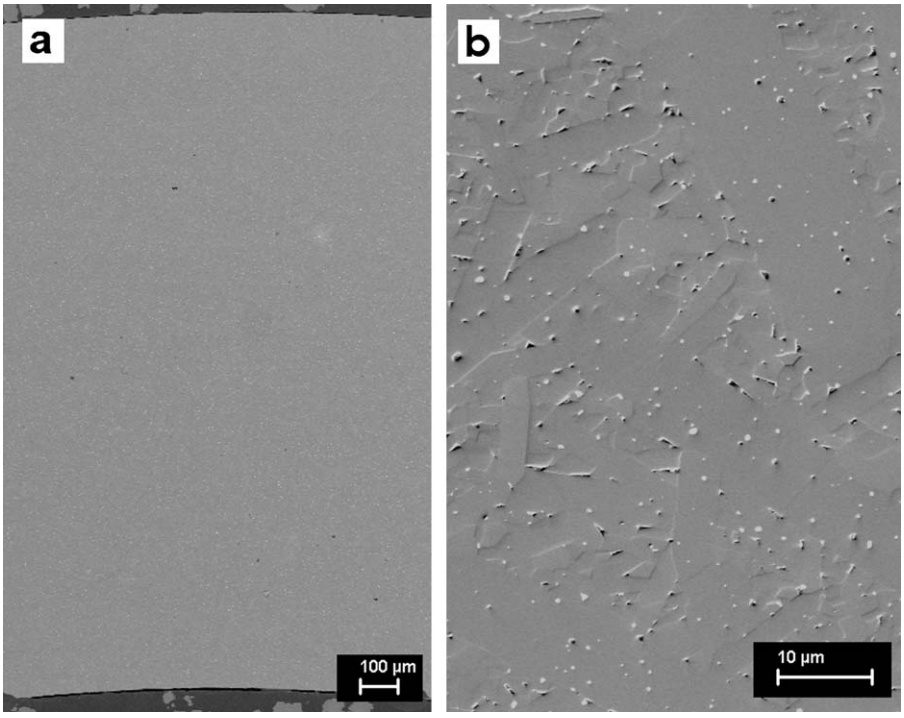

Fig. 9. Microstructure of a sintered α-alumina sample: (a) cross-section through the tube wall, (b) detail of the microstructure.

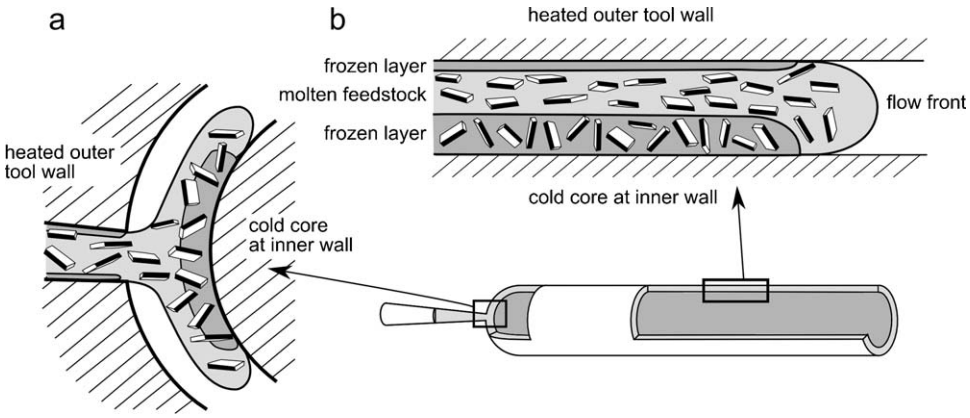

Fig. 10. Particle orientation in the feedstock stream while filling the cavity, (a) the feedstock passes the gate, impinges onto the core and forms a frozen layer, (b) the propagating feedstock fills the tube cavity.

of the flat stacked inner layer is larger than in the outer layer where the particles touch each other frontally with less binder in between. Therefore, stresses are introduced in both areas. If the interface strength is too small they may delaminate. In the opposite case the inner layer is clamped by the less shrinking outer layer and tension forces arise at the inner surface which causes cracks growing into the tube wall. They stop as they reach the parallel particles (Figs. 6 and 8).

During sintering a similar phenomenon can be observed. The differential shrinkage of the inner and outer layer leads to delamination at predamaged sites which are located at the internal interface and causes extended blisters by an outwards bulge. The radial cracks are stopped or deflected at the interface because they follow the grain boundaries[18] or in case of our porous structure the orientated pores.

5. Conclusions

In this study the flow and mould filling behaviour of a feedstock consisting of a highly anisotropic powder with a high specific surface was investigated. The binder system which has been developed proofed to be suited for processing fine grained powders. In case of a spherically shaped α-alumina defect-free samples could be obtained after sintering. However, the morphology of the β-alumina which consists of 20 nm thin platelets makes injection moulding extremely difficult. During mould filling the mobility of the plate-like particles is hindered since they are limited to lateral movement and can hardly rotate which is especially critical when the flow direction changes. Due to the increasing viscosity solid loading was limited to 48 vol.%. In general, feedstocks with such a relatively high binder amount are vulnerable to debinding defects. Additionally, in the β-alumina samples the particles are aligned along the flow pattern which is determined by the specific tool and moulding conditions. Defect formation in debinding and sintering could be related to the particle or grain pattern.

These results point out that the orientation of anisometric powders in injection moulded parts does not only complicate the moulding process itself, but has also serious consequences for the microstructure and quality of the end product. If the use of anisometric powders cannot be omitted the specific feedstock behaviour has to be considered in the component and tool design phase. For example, adjacent layers of different particle orientations should be avoided by preventing frozen layers at the mould surface (variothermal heating). In this way the particles will be oriented uniformly and there will be less stresses in the cross-section of the part during debinding and sintering. However, this involves anisotropic shrinkage and material properties depending on the position relative to the flow direction which has to be accounted for in the component design.

Acknowledgement

The presented study is part of the project “Process innovation and energy saving in the cement and derived fuels applying industry by the use of alkali-corrosion resistant layers and components” which is financed by the German Federal Ministry of Education and Research (BMBF) under the number 03X3527. The following partners are involved in the project: Calsitherm Verwaltungs GmbH, Refratechnik Cement GmbH, Schöler+Bolte Bolzenschweiss-Systeme, Lafarge Zement Karsdorf GmbH, Freiberg University of Mining and Technology, Fraunhofer IKTS and Forschungszentrum Jülich GmbH.

References

1. Lin STP, German RM. The influence of powder loading and binder additive on the properties of alumina injection-moulding blends. *J Mater Sci* 1994;**29**:5367–73.
2. Song JH, Evans JRG. The effect of undispersed agglomerates on the relative viscosity of ceramic moulding suspensions. *J Mater Sci Lett* 1994;**13**:1642–4.
3. Suri P, Atre SV, German RM, deSouza J. Effect of mixing on the rheology and particle characteristics of tungsten-based powder injection molding feedstock. *Mater Sci Eng* 2003;**A356**:337–44.
4. German RM, Bose A. *Injection moulding of metals and ceramics metal powder industries federation*. NJ: Princeton; 1997.
5. Yamamoto S, Matsuoka T. Dynamic simulation of rod-like and plate-like particle dispersed systems. *Comp Mater Sci* 1999;**14**:169–76.
6. Wang K, Zhao P, Yang H, Liang S, Zhang Q, Du R, et al. Unique clay orientation in the injection-molded bar of isotactic polypropylene/clay nanocomposite. *Polymer* 2006;**47**:7103–10.
7. Bernasconi A, Davoli P, Basile A, Filippi A. Effect of fibre orientation on the fatigue behaviour of a short glass fibre reinforced polyamide-6. *Int J Fatigue* 2007;**29**:199–208.

8. Choi W, Kim S. Effects of talc orientation and non-isothermal crystallization rate on crystal orientation of polypropylene in injection-molded polypropylene/ethylene-propylene rubber/talc blends. *Polymer* 2004;**45**:2393–401.
9. Weon J, Sue H. Effects of clay orientation and aspect ratio on mechanical behavior of nylon-6 nanocomposite. *Polymer* 2005;**46**:6325–34.
10. Zhang T, Blackburn S, Bridgwater J. The orientation of binders and particles during ceramic injection moulding. *J Europ Ceram Soc* 1997;**17**:101–8.
11. Zhang T, Blackburn S, Bridgwater J. Debinding and sintering defects from particle orientation in ceramic injection moulding. *J Mater Sci* 1996;**31**:5891–6.
12. Ozer I, Suvaci E, Karademir B, Missiaen J, Carry C, Bouvard D. Anisotropic sintering shrinkage in alumina ceramics containing oriented platelets. *J Am Ceram Soc* 2006;**89**:1972–6.
13. Uematsu K, Ohsaka S, Takahashi H, Shinohara N, Okumiya M, Yokota Y, et al. Characterization of micro- and macrostructure of injection-molded green body by liquid immersion method. *J Eur Ceram Soc* 1997;**17**:177–81.
14. Shui A, Kato Z, Tanaka S, Uchida N, Uematsu K. Sintering deformation caused by particle orientation in uniaxially and isostatically pressed alumina compacts. *J Eur Ceram Soc* 2002;**22**:311–6.
15. Krug S, Evans JRG, ter Maat JHH. Differential sintering in ceramic injection moulding: particle orientation effects. *J Eur Ceram Soc* 2002;**22**:173–81.
16. Wright JK, Edirisinghe MJ, Zhang JG, Evans JRG. Particle packing in ceramic injection molding. *J Am Ceram Soc* 1990;**73**:2653–8.
17. Liu D-M, Tseng WJ. Influence of debinding rate, solid loading and binder formulation on the green microstructure and sintering behaviour of ceramic injection mouldings. *Ceram Int* 1998;**24**:471–81.
18. Sakka Y, Suzuki T, Uchikoshi T. Fabrication and some properties of textured alumina-related compounds by colloidal processing in high-magnetic field and sintering. *J Eur Ceram Soc* 2008;**28**:935–42.